J|A|C|S ARTICLES

Published on Web 08/12/2010

Geminate Charge Recombination in Polymer/Fullerene Bulk Heterojunction Films and Implications for Solar Cell Function

Suman Kalyan Pal,[†,‡] Tero Kesti,[§] Manisankar Maiti,[†] Fengling Zhang,[||] Olle Inganäs,[||] Stefan Hellström,[⊥] Mats R. Andersson,[⊥] Frederic Oswald,[#] Fernando Langa,[#] Tomas Österman,[†] Torbjörn Pascher,[†] Arkady Yartsev,[†] and Villy Sundström*[,†]

Chemical Physics, Lund University, P.O. Box 124, SE-221 00 Lund, Sweden, Measurement and Sensor Laboratory, University of Oulu, 87400 Kajaani, Finland, Biomolecular and Organic Electronics, Department of Physics (IFM), Linköping University, S-581 83 Linköping, Sweden, Department of Chemical and Biological Engineering, Chalmers University of Technology, SE-412 96 Gothenburg, Sweden, and Instituto de Nanociencia, Nanotecnologia y Materiales Moleculares (INAMOL), Universidad de Castilla-La Mancha, Campus de la Fábrica de Armas, Toledo 45071, Spain

Received June 1, 2010; E-mail: Villy.sundstrom@chemphys.lu.se

Abstract: We have studied the influence of three different fullerene derivatives on the charge generation and recombination dynamics of polymer/fullerene bulk heterojunction (BHJ) solar cell blends. Charge generation in APFO3/[70]PCBM and APFO3/[60]PCBM is very similar and somewhat slower than charge generation in APFO3/[70]BTPF. This difference qualitatively matches the trend in free energy change of electron transfer estimated from the LUMO energies of the polymer and fullerene derivatives. The first order (geminate) charge recombination rate is significantly different for the three fullerene derivatives studied and increases in the order APFO3/[70]PCBM < APFO3/[60]PCBM < APFO3/[70]BTPF. The variation in electron transfer rate cannot be explained from the LUMO energies of the fullerene derivatives and single-step electron transfer in the Marcus inverted region and simple considerations of expected trends for the reorganization energy and free energy change. Instead we suggest that geminate charge recombination occurs from a state where electrons and holes have separated to different distances in the various materials because of an initially high charge mobility, different for different materials. In a BHJ thin film this charge separation distance is not sufficient to overcome the electrostatic attraction between electrons and holes and geminate recombination occurs on the nanosecond to hundreds of nanoseconds time scale. In a BHJ solar cell, we suggest that the internal electric field in combination with polarization effects and the dynamic nature of polarons are key features to overcome electron−hole interactions to form free extractable charges.

Introduction

Polymer based organic solar cells have attracted much attention because of their cheap and easy methods of processing.[1−5] Solar cell performances have been improved considerably by making a bulk heterojunction (BHJ)[6,7] of the conjugated polymer (the electron donor) and the electron acceptor.[3] The interpenetrating network of the BHJ increases the interfacial area between the donor and acceptor, resulting in improved solar cell efficiency. Although in this construction, either a second polymer[8,9] or a small molecule[7,10] can be used as an acceptor, fullerenes are widely used because of ultrafast photoinduced electron transfer between the conjugated polymer and fullerene.[11,12] In a polymer/fullerene solar cell, the most commonly used fullerene derivative is [6,6]phenyl-C_{61}-butyric acid methyl ester ([60]PCBM).[13−17] Polymer/fullerene bulk heterojunction solar

[†] Lund University.
[‡] Present address: Department of Chemistry and Center for Photochemical Sciences, Bowling Green State University, Bowling Green, Ohio.
[§] University of Oulu.
[||] Linköping University.
[⊥] Chalmers University of Technology.
[#] Universidad de Castilla-La Mancha.

(1) Brabec, C. J. *Sol. Energy Mater. Sol. Cells* **2004**, *83*, 273–292.
(2) Brabec, C. J.; Sariciftci, N. S.; Hummelen, J. C. *Adv. Funct. Mater.* **2001**, *11*, 15–26.
(3) Coakley, K. M.; McGehee, M. D. *Chem. Mater.* **2004**, *16*, 4533–4542.
(4) Service, R. F. *Science* **2005**, *309*, 548–551.
(5) Tang, C. W. *Appl. Phys. Lett.* **1986**, *48*, 183–185.
(6) Brabec, C. J.; Zerza, G.; Cerullo, G.; De Silvestri, S.; Luzzati, S.; Hummelen, J. C.; Sariciftci, S. *Chem. Phys. Lett.* **2001**, *340*, 232–236.
(7) Yu, G.; Gao, J.; Hummelen, J. C.; Wudl, F.; Heeger, A. J. *Science* **1995**, *270*, 1789–1791.
(8) Halls, J. J. M.; Friend, R. H. *Synth. Met.* **1997**, *85*, 1307–1308.
(9) Halls, J. J. M.; Walsh, C. A.; Greenham, N. C.; Marseglia, E. A.; Friend, R. H.; Moratti, S. C.; Holmes, A. B. *Nature* **1995**, *376*, 498–500.
(10) Dittmer, J. J.; Marseglia, E. A.; Friend, R. H. *Adv. Mater.* **2000**, *12*, 1270–1274.
(11) Sariciftci, N. S.; Smilowitz, L.; Heeger, A. J.; Wudl, F. *Science* **1992**, *258*, 1474–1476.
(12) De, S.; Pascher, T.; Maiti, M.; Jespersen, K. G.; Kesti, T.; Zhang, F. L.; Inganas, O.; Yartsev, A.; Sundstrom, V. *J. Am. Chem. Soc.* **2007**, *129*, 8466–8472.
(13) Yang, X. N.; van Duren, J. K. J.; Janssen, R. A. J.; Michels, M. A. J.; Loos, J. *Macromolecules* **2004**, *37*, 2151–2158.

 10.1021/ja104786x

cells have now been demonstrated to achieve a power conversion efficiency of 6% under AM 1.5 conditions[18] or higher.[19,20]

Often, in BHJs the polymer has the dominant role of light harvesting initiating the charge transfer and transport processes ultimately leading to photocurrent in a solar cell. The following key steps can be anticipated in the photon to current conversion process. Polymer excitons generated by light absorption are converted into bound electron−hole pairs (bound radical pair,[21−24] charge transfer states[25−30]). These bound charge pairs have to dissociate further to form mobile (free) charge carriers. In reported efficient BHJ solar cells, exciton dissociation is typically strongly exoenergetic and occurs with high quantum yield. Nevertheless it has been discussed that some driving force is required for efficient conversion of excitons into charges,[24] but this issue is still not fully clarified. Apparently, for an efficient solar cell, most excitons have to be converted into mobile (free) charge carriers. From realization that the Coulomb interaction between polymer/fullerene charge pairs in close contact is many times higher than the thermal energy, it may be wondered what is the mechanism that separates the bound charges to form mobile charges that doubtlessly must exist in a solar cell with an EQE exceeding 50%. This is one of the questions we will address in this work.

Geminate charge pair recombination (Onsager recombination) to ground state, or back to excited singlet or triplet states, is a loss process decreasing the yield of mobile useful charges. Additionally, the charges that escape Onsager recombination may also recombine. This may occur nongeminately if their density is high enough, but it can also be expected that charge pairs that escaped Onsager recombination and have moved apart can undergo geminate recombination under the influence of the remaining electrostatic attraction. In fact, we will show here that for the polymer APFO3 (poly[2,7-(9,9-dioctylfluorene)-alt-5,5-(4,7′-di-2-thienyl-2′,1′,3-benzothiadiazole)]) and three different fullerene acceptors this is the major recombination channel in a BHJ thin film at low light intensities and it occurs on the nanosecond to hundreds of nanoseconds time scale, much faster than the expected microsecond charge extraction time. In a BHJ solar cell with high IQE this recombination is evidently outcompeted by other processes leading to efficient charge extraction. There is presently not much detailed knowledge on how this happens and which are the underlying mechanisms, but in a recent review Bredas et al.[27] discussed possible scenarios. Here we will provide experimental results that help shed some light on the processes involved. We achieve this by studying the dynamics of charge carriers formed by photoexcitation in APFO3/[70]PCBM ([6,6]phenyl-C_{71}-butyric acid methyl ester) and APFO3/[70]BTPF (3′-(3,5-bis-trifluoromethylphenyl)-1′-(4-nitrophenyl)pyrazolino[70]fullerene) 1:1 blends using femtosecond pump probe and nanosecond flash photolysis techniques and compare these results with the results for an APFO3/[60]PCBM 1:1 blend, reported earlier.[12]

We find that the first order (geminate) recombination of separated charges strongly depends on the type of fullerene derivative in the solar cell blend; the rate is slowing down in going from APFO3/[70]BTPF to APFO3/[60]PCBM to APFO3/[70]PCBM, but the variation of charge recombination times cannot be explained from the LUMO energies of the fullerene derivatives and a single-step electron transfer in the Marcus inverted region and simple considerations of expected trends for the reorganization energy and free energy change. Instead we suggest that geminate charge recombination occurs from a state where electrons and holes have separated to different distances in the various materials because of an initially high charge mobility, different for different materials. We find that geminate charge recombination occurs from a charge separation distance varying from 1.2 to 4.6 nm for the three blends. In the absence of an internal electric field, in the BHJ film, the electrostatic attraction pulls the separated charges back together to undergo first order recombination on the nanosecond to hundreds of nanoseconds time scale. In a functional solar cell we suggest that the dynamic nature of polarons results in a time averaged screening of the charges such that the internal electric field in the solar cell and polarization effects[27] are able to overcome the electrostatic attraction between electrons and holes and allow conversion of bound photogenerated charges into mobile charge carriers.

We also observe that charge generation proceeds with ∼100% efficiency independently of the fullerene used with a generation rate that qualitatively follows the driving force variation. However, the high rates of charge generation, in combination with previously estimated values of the reorganization energy, may indicate that adiabatic electron passage from the excited APFO3 to a fullerene has to be considered for this reaction step.

Experimental Section

Sample Preparation. The structures of the polymer APFO3 and acceptors [70]PCBM and [70]BTPF are shown in Figure 1. To prepare the film sample, glass substrates were cleaned for 5 min at 85 °C with a mixture of deionized water, ammonia (25%), and hydrogen peroxide (28%) (5:1:1 by volume) followed by thorough cleaning with deionized water. The blend of APFO3 with [70]PCBM

(14) Gebeyehu, D.; Brabec, C. J.; Padinger, F.; Fromherz, T.; Hummelen, J. C.; Badt, D.; Schindler, H.; Sariciftci, N. S. *Synth. Met.* **2001**, *118*, 1–9.
(15) Hoppe, H.; Niggemann, M.; Winder, C.; Kraut, J.; Hiesgen, R.; Hinsch, A.; Meissner, D.; Sariciftci, N. S. *Adv. Funct. Mater.* **2004**, *14*, 1005–1011.
(16) Martens, T.; D'Haen, J.; Munters, T.; Beelen, Z.; Goris, L.; Manca, J.; D'Olieslaeger, M.; Vanderzande, D.; De Schepper, L.; Andriessen, R. *Synth. Met.* **2003**, *138*, 243–247.
(17) van Duren, J. K. J.; Yang, X. N.; Loos, J.; Bulle-Lieuwma, C. W. T.; Sieval, A. B.; Hummelen, J. C.; Janssen, R. A. J. *Adv. Funct. Mater.* **2004**, *14*, 425–434.
(18) Kim, K.; Liu, J.; Namboothiry, M. A. G.; Carroll, D. L. *Appl. Phys. Lett.* **2007**, *90*, 163511.
(19) Chen, H. Y.; Hou, J. H.; Zhang, S. Q.; Liang, Y. Y.; Yang, G. W.; Yang, Y.; Yu, L. P.; Wu, Y.; Li, G. *Nat. Photonics* **2009**, *3*, 649–653.
(20) Hou, J. H.; Chen, H. Y.; Zhang, S. Q.; Chen, R. I.; Yang, Y.; Wu, Y.; Li, G. *J. Am. Chem. Soc.* **2009**, *131*, 15586–15587.
(21) Gulbinas, V.; Zaushitsyn, Y.; Sundstrom, V.; Hertel, D.; Bassler, H.; Yartsev, A. *Phys. Rev. Lett.* **2002**, *89*, 107401.
(22) Gulbinas, V.; Zaushitsyn, Y.; Bassler, H.; Yartsev, A.; Sundstrom, V. *Phys. Rev. B* **2004**, *70*, 035215.
(23) Zaushitsyn, Y.; Gulbinas, V.; Zigmantas, D.; Zhang, F. L.; Inganas, O.; Sundstrom, V.; Yartsev, A. *Phys. Rev. B* **2004**, *70*, 075202.
(24) Ohkita, H.; Cook, S.; Astuti, Y.; Duffy, W.; Tierney, S.; Zhang, W.; Heeney, M.; McCulloch, I.; Nelson, J.; Bradley, D. D. C.; Durrant, J. R. *J. Am. Chem. Soc.* **2008**, *130*, 3030–3042.
(25) Bakulin, A. A.; Martyanov, D.; Paraschuk, D. Y.; van Loosdrecht, P. H. M.; Pshenichnikov, M. S. *Chem. Phys. Lett.* **2009**, *482*, 99–104.
(26) Benson-Smith, J. J.; Goris, L.; Vandewal, K.; Haenen, K.; Manca, J. V.; Vanderzande, D.; Bradley, D. D. C.; Nelson, J. *Adv. Funct. Mater.* **2007**, *17*, 451–457.
(27) Bredas, J. L.; Norton, J. E.; Cornil, J.; Coropceanu, V. *Acc. Chem. Res.* **2009**, *42*, 1691–1699.
(28) Hwang, I. W.; Moses, D.; Heeger, A. J. *J. Phys. Chem. C* **2008**, *112*, 4350–4354.
(29) Tvingstedt, K.; Vandewal, K.; Gadisa, A.; Zhang, F. L.; Manca, J.; Inganas, O. *J. Am. Chem. Soc.* **2009**, *131*, 11819–11824.
(30) Veldman, D.; Ipek, O.; Meskers, S. C. J.; Sweelssen, J.; Koetse, M. M.; Veenstra, S. C.; Kroon, J. M.; van Bavel, S. S.; Loos, J.; Janssen, R. A. J. *J. Am. Chem. Soc.* **2008**, *130*, 7721–7735.

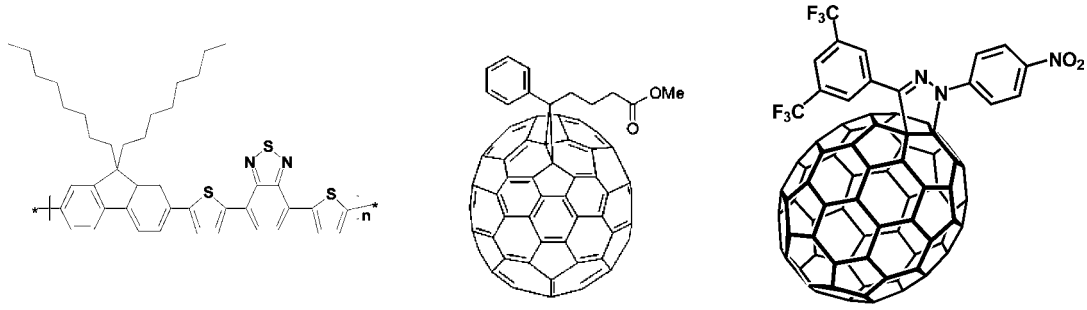

APFO3 [70]PCBM [70]BTPF

Figure 1. Structures of APFO3 and C_{70}-fullerene based acceptors.

was spin-coated on cleaned glass substrates from chloroform solutions in a 1:1 stoichiometry (by weight). The films of APFO3 mixed with [70]BTPF in the same stoichiometry were cast from a mixed solution of chloroform and dichlorobenzene in the ratio of 4:1 (by volume) due to poor solubility of [70]BTPF in neat chloroform. In order to avoid oxidation of the samples, the blend films were encapsulated with another clean glass substrate using melted plastic as glue, inserted between the two glass substrates at the edges and heated to about 100 °C. Solar cells based on the same polymer/fullerene combinations were fabricated and characterized under conditions described elsewhere.[31]

Steady-State and Time-Resolved Spectroscopic Measurements. Steady-state absorption spectra were measured in an Agilent 8453 UV−visible spectrophotometer and steady-state fluorescence spectra were measured with a Spex Fluorolog 1681 spectrometer. Transient absorption (TA) studies with 30 fs pulses were performed using an experimental setup based on a commercial 1 kHz Clark MXR CPA 2001 fs laser, pumping a noncollinear optical parametric amplifier (Clark MXR Inc., NOPA) to generate the probe pulses. Another amplifier (TOPAS White, Light Conversion) was used for generation of pump pulses at 580 and 535 nm. TA kinetics was measured by detection of undispersed probe and reference pulses. The probe components polarized parallel ($\Delta A_{\parallel}$) and perpendicular ($\Delta A_{\perp}$) to the pump polarization were detected simultaneously but independently. Experiments were performed using both short (500 ps, 30 fs instrumental function) and long (10 ns, ~1 ps resolution) delay lines. Kinetics at even longer times was measured with a nanosecond TA setup with 6 ns resolution, described elsewhere.[32] In these experiments, the samples were excited at 580 nm and an unfocused helium−neon laser (543 nm) was used to probe the kinetics. Time correlated single photon counting fluorescence measurements were performed using a PicoQuant PicoHarp 300, exciting with a 405 nm picosecond laser (PicoQuant Sepia II PDL 828) and detecting with a single photon avalanche diode (Micro Photon Devices PDM 100CT). Filters were used to select the wavelength of interest.

Electrochemical Measurements. Square-wave voltammetry measurements[33] were carried out on a CH-Instruments 650A electrochemical workstation. A three-electrode setup consisting of platinum wires as both working electrode and counter electrode and an Ag/Ag^+ quasi reference electrode was used. A solution of tetrabutylammonium hexafluorophosphate (Bu_4NPF_6) in anhydrous acetonitrile/*o*-dichlorobenzene (1:4) (0.1 M) was used as supporting electrolyte. The polymer and fullerene derivatives were dissolved in the electrolyte solution. The electrolyte was bubbled with nitrogen gas prior to each experiment. During the scans, nitrogen gas was flushed over the electrolyte surface. After each experiment, the system was calibrated by measuring the ferrocene/ferrocenium (Fc/Fc^+) redox peak. The HOMO and LUMO energy levels of the polymers and electron acceptors were calculated from the peak values of the third scan by setting the oxidative peak potential of Fc/Fc^+ vs the normal hydrogen electrode (NHE) to 0.630 V [34] and the NHE vs the vacuum level to 4.5 V.[35]

Modeling. The modeling of the kinetic data was performed using the Nelder−Mead simplex method for the rate constants and using general linear regression for the amplitudes as described earlier.[36] In order to cover the time window of 30 fs to 50 μs three sets of data, femtosecond kinetics for both the short (500 ps) and long (10 ns) delay line and nanosecond kinetics, were used. For all blends, the femtosecond kinetics used for fitting covered the excitation intensity range $10^{12}-10^{14}$ (ph/cm^2)/pulse (ph = photons) (for APFO3/[70]PCBM, eight measurements at various intensities with both short and long delay lines (four of each), and for APFO3/[70]BTPF three measurements of each time range, Figure 8i and Figure SI3), whereas one nanosecond data set was used. For each blend, all kinetic traces were fitted simultaneously in a global fashion, yielding a coherent picture of relative contribution of first and second order processes. In the fitting procedure, the data were weighted to put emphasis on the low intensity traces such that small relative errors in the high intensity traces would not dominate the fit. Likewise, errors from the femtosecond part were given more weight than errors from the nanosecond part so that noise in the early part of the nanosecond traces would not influence the fitted rates.

Results

Steady-State Absorption and Fluorescence Measurements. The absorption spectra of neat APFO3, neat [70]PCBM, neat [70]BTPF, AFO3/[70]PCBM 1:1 blend, and APFO3/[70]BTPF 1:1 blend are shown in Figure 2. The absorption spectrum of [70]PCBM has a long tail extending up to ~725 nm and is very much similar to the absorption spectrum of [70]BTPF. The absorption spectrum of neat APFO3 has two separate peaks at 384 and 540 nm. Polymer/fullerene 1:1 blends (APFO3/[70]PCBM and APFO3/[70]BTPF) show significant absorption up to ~725 nm. Figure 3 shows the fluorescence spectra of neat polymer and 1:1 blends of APFO3/[70]PCBM and APFO3/[70]BTPF. The fluorescence spectra of blends show that the fluorescence of neat polymer is reduced by more than 2 orders of magnitude, which indicates strong quenching of polymer

(31) Zhang, F. L.; Mammo, W.; Andersson, L. M.; Admassie, S.; Andersson, M. R.; Inganas, L.; Admassie, S.; Andersson, M. R.; Ingands, O. *Adv. Mater.* **2006**, *18*, 2169–2173.
(32) Pascher, T. *Biochemistry* **2001**, *40*, 5812–5820.
(33) Osteryoung, J. G.; Osteryoung, R. A. *Anal. Chem.* **1985**, *57*, A101.
(34) Pavlishchuk, V. V.; Addison, A. W. *Inorg. Chim. Acta* **2000**, *298*, 97–102.
(35) Bard, A. J.; Faulkner, L. R. *Electrochemical Methods: Fundamentals and Applications*; Wiley: New York, 1980.
(36) Beechem, J. M. *Methods Enzymol.* **1992**, *210*, 37–54.

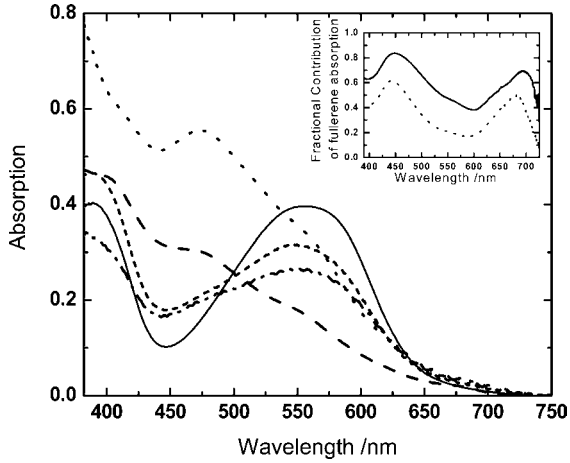

Figure 2. Absorption spectra of neat APFO3 (solid line), neat [70]PCBM (dotted line), neat [70]BTPF (dashed line), APFO3/[70]PCBM 1:1 blend (dash-dotted line), and APFO3/[70]BTPF 1:1 blend (short-dashed line). Inset: fractional contribution of [70]PCBM (solid line) and [70]BTPF (dotted line) absorption in polymer/fullerene blends.

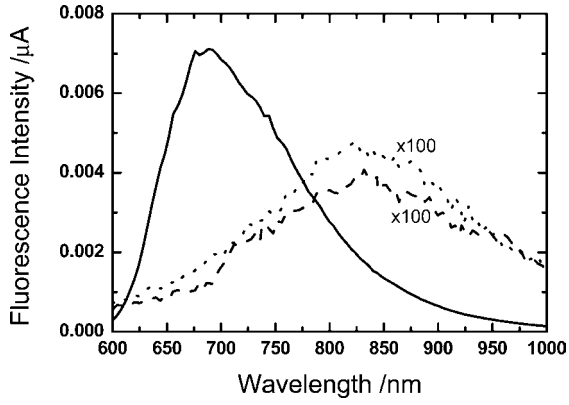

Figure 3. Fluorescence spectra of neat APFO3 film (solid line) and APFO3/[70]PCBM 1:1 blend (dotted line) at excitation wavelength 580 nm and APFO3/[70]BTPF 1:1 blend (dashed line) at excitation wavelength 535 nm.

fluorescence in the presence of the fullerene derivative. In the blends, however, a new band at ∼825 nm is observed. Such emission has been reported for similar polymer/fullerene blends and attributed to emission from a CT state.[30,37] Because of overlapping of quenched emission of neat polymer and CT emission, it is hard to estimate the fluorescence quantum yield of the CT emission. The maximum value of the relative fluorescence quantum yield of the CT emission is 1% for the 1:1 blend of APFO3/[70]PCBM and 0.8% for the 1:1 blend of APFO3/[70]BTPF, with respect to neat APFO3. Further characterization of the CT state for several polymer/fullerene blend films has been performed very recently.[25,29,30,38−41]

Electrochemistry of the Constituent Components. Information about the energies of HOMO and LUMO levels of the polymer and fullerene derivatives is generally available from electrochemistry measurements, and values have been published.[42,43] However, it is well-known that it may be difficult to compare results obtained in different measurements; therefore, we measured the HOMO and LUMO energies of APFO3 and the fullerene derivatives used in the experiments, employing the square-wave voltammetry technique. The obtained values are summarized in Table 1 and will be used when we discuss and compare the measured rates of charge generation and recombination in the APFO3/fullerene blends.

Table 1. HOMO and LUMO Energies of APFO3 and Fullerene Derivatives Measured by Square-Wave Voltammetry

	HOMO (eV)	LUMO (eV)
[60]PCBM	−6.2	−4.0
[70]PCBM	−6.2	−4.0
[70]BTPF	−6.3	−4.2
APFO3	−5.6	−3.4

TA Spectra of Neat APFO3 and APFO3/Fullerene Blends. Transient absorption (TA) spectra of neat APFO3 have three features: the ground state bleach at 570 nm, the stimulated emission at around 700 nm, and a positive band at ∼900 nm mainly due to excited state absorption of the polymer with minor contribution from charge carriers formed after photoexcitation of APFO3.[12] Transient spectra of APFO3/fullerene blends exhibit the ground state bleach at nearly the same wavelength as that of the neat polymer and a broad absorption band (650−1000 nm) due to positive charges residing on the polymer.[12,44] No stimulated emission from the polymer was observed in the polymer/fullerene blends studied here because of strong fluorescence quenching. These spectral characteristics of excited state and charged species imply that the wavelength region around 1000 nm can be used to probe the formation of the polymer excited state, its decay, and concomitant formation of the charged species.[12] The decay of the 1000 nm signal at later times characterizes the disappearance of charges (recombination). TA kinetics of the recovery of ground state bleach of neat polymer is identical to the TA decay observed at 1000 nm,[12] showing that recombination leads to direct formation of the ground state without intervening intermediates. Charge recombination can therefore be monitored by probing at ground state bleach region (∼570 nm). Thus, the TA kinetics of the 1:1 blends of APFO3/[70]PCBM and APFO3/[70]BTPF films were measured by probing at 1000 nm up to 500 ps and 10 ns and probing at 543 nm up to 50 μs (Figure 4) to monitor the complete "life cycle" of photoexcitations, from formation of polymer excitons to recombination of charges. In conjugated polymers spectral signatures of separated charges (isolated polarons) have previously been shown to differ from those of bound charge pairs (polaron pairs);[45] therefore, following the spectral characteristics of charged species we may expect to observe dynamic features correlated to the process of spatial separation of photogenerated charges.

TA Kinetics of APFO3/[70]PCBM and APFO3/[70]BTPF Blends. The TA kinetics of the 1:1 blends of APFO3/[70]PCBM and APFO3/[70]BTPF measured at a pump intensity of ∼10^{13}

(37) Loi, M. A.; Toffanin, S.; Muccini, M.; Forster, M.; Scherf, U.; Scharber, M. *Adv. Funct. Mater.* **2007**, *17*, 2111–2116.
(38) Hallermann, M.; Kriegel, I.; Da Como, E.; Berger, J. M.; von Hauff, E.; Feldmann, J. *Adv. Funct. Mater.* **2009**, *19*, 3662–3668.
(39) Vandewal, K.; Tvingstedt, K.; Gadisa, A.; Inganas, O.; Manca, J. V. *Nat. Mater.* **2009**, *8*, 904–909.
(40) Vandewal, K.; Tvingstedt, K.; Gadisa, A.; Inganas, O.; Manca, J. V. *Phys. Rev. B* **2010**, *81*, 125204.
(41) Zhou, Y.; Tvingstedt, K.; Zhang, F. L.; Du, C. X.; Ni, W. X.; Andersson, M. R.; Inganas, O. *Adv. Funct. Mater.* **2009**, *19*, 3293–3299.
(42) Wang, X. J.; Perzon, E.; Oswald, F.; Langa, F.; Admassie, S.; Andersson, M. R.; Inganas, O. *Adv. Funct. Mater.* **2005**, *15*, 1665–1670.
(43) Andersson, L. M.; Inganas, O. *Appl. Phys. Lett.* **2006**, *88*, 082103.
(44) Jespersen, K. G.; Zhang, F. L.; Gadisa, A.; Sundstrom, V.; Yartsev, A.; Inganas, O. *Org. Electron.* **2006**, *7*, 235–242.
(45) Lane, P. A.; Wei, X.; Vardeny, Z. V. *Phys. Rev. B* **1997**, *56*, 4626–4637.

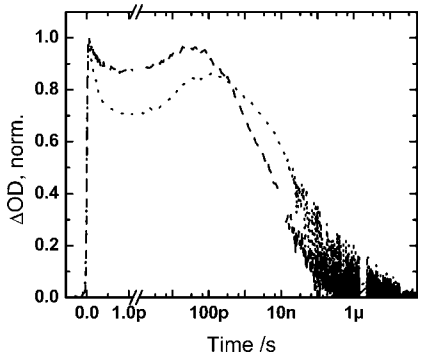

Figure 4. TA kinetics of a 1:1 APFO3/[70]PCBM blend at laser fluence of $\sim 5.3 \times 10^{13}$ (ph/cm^2)/pulse (dotted line) and TA kinetics of a 1:1 blend of APFO3/[70]BTPF at laser fluence of $\sim 7.5 \times 10^{13}$ (ph/cm^2)/pulse (dashed line). The time axis (abscissa) is linear up to ~1 ps and logarithmic later on.

(ph/cm^2)/pulse are shown in Figure 4. The kinetic traces have three regions: (i) an initial ultrafast decay, (ii) a rise, and (iii) a relatively slow decay. Similar TA kinetics was observed in APFO3/[60]PCBM blends containing high [60]PCBM concentrations (1:1 to 1:4 APFO3/[60]PCBM).[12] At the excitation wavelengths of the TA measurements (580 nm for APFO3/[70]PCBM and 535 nm for APFO3/[70]BTPF), the C_{70}-fullerene derivatives have significant ground state absorption (inset of Figure 2), implying that the C_{70}-fullerene derivatives may contribute to the TA kinetics of the polymer/fullerene blends at 1000 nm. There are two possibilities: excitation of the fullerene gives rise to a TA response similar to that of neat fullerene; fullerene excitation leads to an excitation that eventually ends up on the polymer. In the second case, dynamics could be different from that with polymer excitation. The first possibility can be discarded, since the TA signals of the neat C_{70}-fullerene derivatives are very weak compared to that of the blends at 1000 nm (data not shown). The second possibility was examined by measuring the TA kinetics of the APFO3/[70]PCBM blend at three different excitation wavelengths with different polymer/[70]PCBM absorbance ratios (530, 580, and 700 nm). The kinetics measured at 1000 nm (see Supporting Information Figure SI1) are identical for all three excitation wavelengths, apart from some minor differences at short times (<10 ps). This shows that the kinetics representing charge separation and recombination, which are the main topic of this paper, does not depend on whether polymer or fullerene is excited initially.

Steady-state fluorescence measurements (Figure 3) showed that the polymer fluorescence is strongly quenched in the blends. On the basis of this strong fluorescence quenching and following the assignment made in our earlier work,[12] we assign the initial ultrafast TA decay to charge transfer from excited polymer to fullerene (monitored by the polymer exciton decay), forming a bound electron−hole pair. The very efficient polymer fluorescence quenching and ultrafast (100−200 fs; see Table 2) charge generation in the blends studied here show that all polymer excitations are directly quenched by charge transfer to the fullerene before any energy transfer in the polymer has occurred; the charge transfer time is at least an order of magnitude shorter than a single energy transfer step in the polymer.[12,46] This shows that no extended regions of neat polymer exist in the studied blends, but they are rather homogeneously mixed. The picosecond rise in the TA kinetics is assigned to the separation of charges in the initially formed Coulomb bound charge pairs to form more loosely bound charge pairs at greater separation distances.[12] We associate the charge separation with an increase of absorptivity of charges (most probably, holes) when they are loosely bound.[45] By analysis of the excitation intensity dependence of the charge recombination and comparison of geminate and nongeminate recombination rates, we will provide more insight into this separation process (below). On a slower nanosecond time scale the separated charges then recombine producing the decay in the TA kinetics.

Table 2. Values of Parameters of Modeling for 1:1 Polymer/Fullerene Blends

	APFO3/[70]PCBM	APFO3/[60]PCBM	APFO3/[70]BTPF
$k_1 \times 10^{-12}$ [a]	4.8	4.8	10.4
$k_2 \times 10^{-10}$ [a]	3.1	3.4	2.1
σ_2 [b]	17		
$k_3 \times 10^{-7}$ [a]	0.3	3.4	15.1
σ_3 [b]	7.3	7.3	42.5
$\gamma_{01} \times 10^{-13}$ [a,c]	5.3	6.6	0.6
α_1	1.01	0.23	1.47
$\gamma_{02} \times 10^{-11}$ [a,c]	2.1	4.6	0.09
α_2	0.83	1.06	2.20
$\varepsilon_{\text{singlet}}$ [d]	1.00	1.00	1.00
$\varepsilon_{\text{charge pair}}$	0.64	0.63	0.87
$\varepsilon_{\text{charge}}$	0.90	0.81	1.13
ε	8.01		

[a] k_1, k_2, and k_3 are given in s^{-1}. γ_{01} and γ_{02} are given in M^{-1} s^{-1}. [b] σ represents the factor in the rate constants k_2 and k_3 corresponding to 1σ in log k Gaussian distribution. [c] γ_{01} and γ_{02} are referenced at 1 ps and 1 ns. $\gamma_1(t) = \gamma_{01}/(t \times 10^{12})^{\alpha 1}$, $\gamma_2(t) = \gamma_{02}/(t \times 10^{9})^{\alpha 2}$ with t in seconds. [d] Set $\varepsilon_{\text{singlet}}$ to 1 in the model.

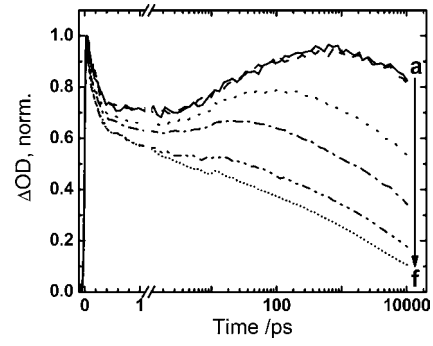

Figure 5. TA kinetics for a 1:1 blend of APFO3/[70]PCBM at various excitation fluences ((ph/cm^2)/pulse): (a) 3.3×10^{12}, (b) 6.6×10^{12}, (c) 5.3×10^{13}, (d) 1.2×10^{14}, (e) 3.3×10^{14}, (f) 6.6×10^{14}. The time axis (abscissa) is linear up to ~1 ps and logarithmic later on.

The charge carrier dynamics in polymer/fullerene solar cell blends depend on the carrier concentration and therefore may have some incident light fluence dependence. The fluence dependence of the TA kinetics (for both APFO3/[70]PCBM and APFO3/[70]BTPF) was studied by varying the excitation intensity over more than 2 orders of magnitude. The kinetics for the 1:1 blend of APFO3/[70]PCBM measured at different excitation intensities are shown in Figure 5 (the corresponding results for APFO3/[70]BTPF are given in Supporting Information (Figure SI2), and for APFO3/[60]PCBM], they can be found in ref 12). For all three blends, at low fluence, the kinetics become intensity independent, showing that recombination under these excitation conditions is of first order and thus geminate in nature. For reasons that we discuss below, the limiting intensity when kinetics become intensity independent is different for the different blends (APFO3/[70]BTPF, $\sim 7.5 \times 10^{13}$ ph

(46) De, S.; Kesti, T.; Maiti, M.; Zhang, F.; Inganas, O.; Yartsev, A.; Pascher, T.; Sundstrom, V. *Chem. Phys.* **2008**, *350*, 14–22.

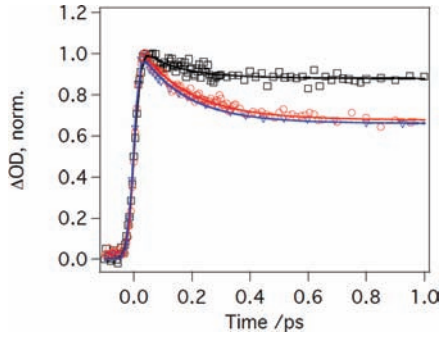

Figure 6. TA kinetics at early time for a 1:1 blend of APFO3/[70]PCBM (▽), APFO3/[60]PCBM (○), and APFO3/[70]BTPF (□) at an excitation photon fluence of 5.3×10^{13} (ph/cm^2)/pulse and their corresponding fits (solid lines).

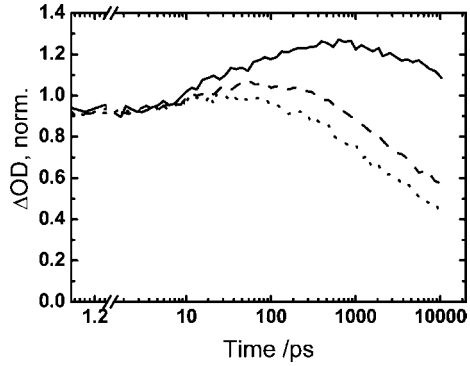

Figure 7. TA kinetics for a 1:1 blend of APFO3/[70]PCBM (solid line), APFO3/ [60]PCBM (dashed line), and APFO3/[70]BTPF (dotted line) at an excitation photon fluence of 3.3×10^{12}, 2.3×10^{13}, and 7.5×10^{12} (ph/cm^2)/pulse, respectively. In each case the fluence is such that the measured kinetics is independent of excitation intensity and thus charge recombination of geminate nature. The time axis (abscissa) is linear up to ~1.2 ps and logarithmic later on.

cm^{-2} pulse^{-1}; APFO3/[60]PCBM], $\sim 3 \times 10^{13}$ ph cm^{-2} pulse^{-1}; APFO3/[70]PCBM, $\sim 6.6 \times 10^{12}$ ph cm^{-2} pulse^{-1}). Both first order geminate and nongeminate recombination involves mobile charges, and the first order recombination involves the electron and hole formed by the same photon. This mode of recombination dominates when the concentration of mobile charges is very low. Intensity dependent behavior is observed at higher fluences as a result of intensity-dependent nongeminate recombination.[12]

TA kinetics at early times (up to 1 ps) for APFO3/[70]PCBM, APFO3/[60]PCBM, and APFO3/[70]BTPF 1:1 blends at an excitation fluence of 5.3×10^{13} (ph/cm^2)/pulse are shown in Figure 6. From the kinetic fitting of these kinetic traces, including deconvolution for the response function, it is clear that the charge formation rates in APFO3/[70]PCBM and APFO3/[60]PCBM are almost the same but somewhat faster in APFO3/[70]BTPF compared to the other two blends (time constants are summarized in Table 2). Figure 7 shows the TA kinetics for blends of APFO3/[70]PCBM, APFO3/[60]PCBM, and APFO3/[70]BTPF probed at 1000 nm, in each case measured at sufficiently low excitation fluence to eliminate nongeminate charge recombination. The kinetic traces show that charge recombination starts very early for the APFO3/[70]BTPF blend compared to the other two blends. At 10 ns, the signal amplitude for APFO3/[70]PCBM blend is higher than that for the APFO3/[60]PCBM and APFO3/[70]BTPF blends. The decay rate of the TA signal is seen to increase in the order APFO3/[70]PCBM < APFO3/[60]PCBM < APFO3/[70]BTPF.

Scheme 1

$$S_0 + h\nu \longrightarrow S_1 \qquad \text{photoexcitation}$$

$$S_1 \xrightarrow{k_1} [e^- : h^+] \qquad \text{charge generation}$$

$$[e^- : h^+] \xrightarrow{k_2} e^- + h^+ \qquad \text{charge separation}$$

$$e^- + h^+ \xrightarrow{k_3} S_0 \qquad \text{geminate recombination}$$

$$[e^- : h^+] + [e^- : h^+] \xrightarrow{\gamma_1} S_0 + [e^- : h^+] \qquad 2^{nd} \text{ order charge pair recombination}$$

$$e^- + h^+ \xrightarrow{\gamma_2} S_0 \qquad \text{nongeminate recombination}$$

From these observations, it is evident that the charge recombination rates are different for different polymer/fullerene blends and the rate increases in going from the blend containing [70]PCBM to [60]PCBM to [70]BTPF.

Modeling of Measured TA Kinetics. As we discussed in relation to Figure 4, the main processes monitored by the TA kinetics of APFO3/[70]PCBM and APFO3/[70]BTPF 1:1 blends are charge generation, charge separation, and first order geminate charge recombination (Scheme 1). We have fitted the TA kinetics for APFO3/[70]BTPF based on Scheme 1 and the model that we used in our earlier APFO3/[60]PCBM work.[12] In that model, charge generation was monitored through the polymer excitonic decay and fitted with a single exponential having rate constant k_1, and the charge separation process was fitted with a single exponential rise having rate constant k_2; the first order charge recombination process fitted well by using a Gaussian distribution in log k_3 space with mean rate constant k_3. The origin of the distributed rate may be a distribution either of electron transfer activation energies or of electron transfer distance, due to material disorder in the polymer/fullerene blends for the long time scale processes.

In order to incorporate the intensity dependence of the recombination kinetics observed at high intensities (Figure 5), a second order nongeminate recombination process (Scheme 1) was added to the model. Also at high intensities, another second order process, charge pair recombination (Scheme 1) occurring on the picosecond time scale, was taken into consideration.[12] The second order processes were fitted with a time dependent rate of the form $\gamma(t) = \gamma_0/t^{\alpha}$. Because of this excitation intensity dependence of the nongeminate charge recombination and charge pair recombination, at high intensity a small fraction of "early" separated charges may recombine nongeminately. In order to visualize the interplay between the various processes describing the charge carrier dynamics in the blend (Scheme 1), we have, on the basis of the fitting results, calculated the turnover rates for each process as a function of excitation intensity for one of the blends (1:1 APFO3/[70]PCBM) at two different times 1 and 10 ps (Figure SI6, parts a and b, respectively), where the difference between rates is smallest and therefore the effect of competition between processes largest. The results show that nongeminate recombination (controlled by γ_2) at all intensities and both times is more than an order of magnitude slower than charge separation (controlled by k_2) (at 1 ps much more than that). Only at the very highest intensities (10^{14} (photons/cm^2)/pulse and higher) the direct charge-pair recombination (controlled by γ_1) has a turnover rate comparable to that of charge separation. This is of course a result of the high charge densities and short intercharge distances at these high excitation intensities; here the charge density is so high that charge pair recombination occurs directly from the initially formed charge pairs, without much time (and need) for charge migration. This result implies

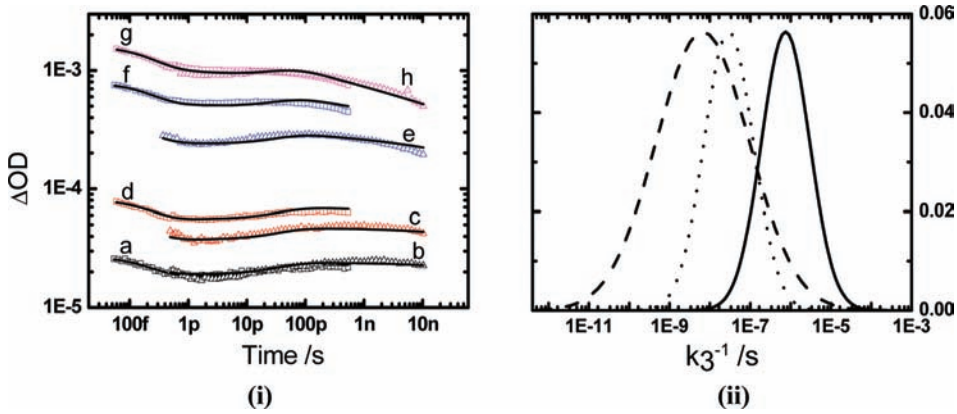

Figure 8. (i) TA kinetics for a 1:1 blend of APFO3/[70]PCBM measured by pump−probe experiments with 500 ps (squares) and 20 ns (triangles) delay line at excitation fluences ((ph/cm^2)/pulse) of (a) 3.2×10^{12}, (b) 3.3×10^{12}, (c) 6.6×10^{12}, (d) 2.4×10^{13}, (e) 5.3×10^{13}, (f) 9.7×10^{13}, (g) 1.3×10^{14}, and (h) 1.2×10^{14}. The solid lines are fits to the data. (ii) Gaussion distribution of the first order geminate recombination time ($1/k_3$) for APFO3/[70]PCBM (solid line), APFO3/[60]PCBM (dotted line), and APFO3/[70]BTPF (dashed line) 1:1 blends. The time axes (abscissa) are logarithmic for both (i) and (ii).

that, except for the very highest excitation intensities used here, the charge separation process is basically complete before charge recombination commences.

Here it is pointed out that in the case of an inhomogeneous material like a BHJ film where distribution of donor−acceptor distances can be expected, it is probably the rule rather than the exception that energy and electron transfer processes are characterized by a distribution of rates. Whether this distribution is uncovered in the experiment and analysis of the kinetic data depends on several factors, signal-to-noise in the measurement, relative magnitude of rate constants, associated amplitudes, etc. To fit the TA kinetics of APFO3/[70]PCBM, a Gaussian distribution of the rates for charge separation and second order recombination was introduced into the model used for the APFO3/[60]PCBM blend. Since the first order charge recombination dynamics in APFO3/[70]PCBM is much slower than for the other blends, the charge separation has time to "express" its distributed rate nature. Figure 8i shows the fits to the measured kinetics for the 1:1 blend of APFO3/[70]PCBM. The corresponding results for APFO3/[70]BTPF are shown in the Supporting Information (Figure SI3).

The results of kinetic modeling for APFO3/[70]PCBM and APFO3/[70]BTPF are summarized in Table 2 along with the corresponding APFO3/[60]PCBM results. It should once more be emphasized that the kinetic modeling, and thus the data in Table 2, for all blends was performed in a global fashion including data taken over 2 orders of magnitude in excitation intensity (see section "Modeling" above). The charge transfer times for APFO3/[70]PCBM and APFO3/[70]BTPF blends are ~200 fs ($k_1 \approx 4.8 \times 10^{12}$ s^{-1}) and ~100 fs ($k_1 \approx 10.4 \times 10^{12}$ s^{-1}), respectively. Charge separation in the APFO3/[70]PCBM blend was fitted with a Gaussian distribution of rates with a mean rate of 3.1×10^{10} s^{-1} and width $\sigma_2 = 17$, unlike what was done for APFO3/[70]BTPF and APFO3/[60]PCBM, where a single exponential rate constant suffices for a good fit. As discussed above, this difference should not be viewed as a difference in relaxation model but rather as a result of differently expressed deviations from single exponential behavior due to the inherent inhomogeneous nature of the materials. In addition, the time scale of separated charge formation is almost the same (~30 ps) for all three polymer/fullerene blends. The modeling results show that the mean geminate recombination time for APFO3/[70]PCBM (~330 ns) is very long compared to that for APFO3/[60]PCBM (~30 ns) and APFO3/[70]BTPF (~7 ns). The width (σ_3) of the Gaussian distribution of the first order recombination rate is large for APFO3/[70]BTPF compared to the other two blends. Plots of the Gaussian distributions of the first order recombination rates for all the blends (Figure 8ii) show that the recombination process starts very early for the APFO3/[70]BTPF blend compared to the other two blends. The nongeminate recombination rate (γ_{02}), which may be a measure of local mobility of charge carriers, is lower for the APFO3/[70]BTPF blend compared to the other two polymer/fullerene blends. Although this may be related to the poor solar cell performance of this material, we refrain from further discussion of this result, since it was obtained under conditions far from those of solar cell operation (extensive second order recombination).

Figure 6 and also the modeling results show that the charge formation process is very fast in the studied polymer/fullerene blends. In order to obtain an accurate charge formation rate, the early time TA kinetics (up to 1 ps) for the three APFO3/fullerene blends were fitted by a single exponential decay including deconvolution with the instrument response function. This procedure yielded the same charge formation rate (~200 fs) for APFO3/[70]PCBM and APFO3/[60]PCBM but approximately twice higher rate (~100 fs) for APFO3/[70]BTPF. TA kinetics at relatively low fluence (~10^{13} (ph/cm^2)/pulse) were used for these fits to avoid the effect of nonlinear processes. In neat polymer film where energy transfer over large distances may occur, exciton−exciton annihilation is an important nonlinear process that may contribute to the excited state decay if too high excitation intensity is used.[47] The time scale of the annihilation process is related to the characteristic time scale of energy transfer, typically picoseconds and longer.[47] For the BHJ films studied here the very efficient fluorescence quenching (Figure 3) and ultrafast charge generation times (Figure 6) show that there are no extended regions of neat polymer in the blend, implying that long-range energy transfer, the prerequisite for exciton−exciton annihilation, does not exist. The very short charge transfer time, much shorter than typical single-step energy transfer, in addition implies that no energy transfer in the polymer can occur before charge formation. For all these

(47) Scheblykin, I. G.; Yartsev, A.; Pullerits, T.; Gulbinas, V.; Sundstrom, V. *J. Phys. Chem. B* **2007**, *111*, 6303–6321.

reasons exciton−exciton annihilation is not an issue under the experimental conditions used here and for the studied BHJ films.

Discussion

Charge Generation Process. We start the discussion with the charge generation process in the different polymer/fullerene blends. Fitting of TA kinetics up to 1 ps by deconvolution shows that the electron transfer (ET) rate for APFO3/[70]PCBM, within experimental error, is the same as that of APFO3/[60]PCBM but lower than that of APFO3/[70]BTPF. Below we discuss the difference in the electron transfer rates on the basis of the Marcus picture of ET.

According to Marcus theory[48] of electron transfer, the rate can be expressed as follows,[49]

$$k_{ET} = \frac{2\pi}{\hbar}|H_{AB}|^2 \frac{1}{\sqrt{4\pi\lambda k_B T}} \exp\left[-\frac{(\Delta G^0 + \lambda)^2}{4\lambda k_B T}\right] \qquad (1)$$

where k_{ET} is the rate of electron transfer, $|H_{AB}|$ is the electronic coupling between the initial and final states, λ is the reorganization energy, and ΔG^0 is the total Gibbs free energy change for the electron transfer reaction (k_B is the Boltzmann constant). The highest occupied molecular orbital (HOMO) and lowest unoccupied molecular orbital (LUMO) energies of APFO3 are −5.6 and −3.4 eV, respectively (Table 1). The LUMO energies of [70]PCBM and [60]PCBM are same (−4.0 eV), but the LUMO energy of [70]BTPF is different (−4.2 eV) (Table 1). Thus, provided that the LUMO energies of the neat materials are good measures of the donor and acceptor LUMOs also in blends, the free energy change (ΔG^0) of forward electron transfer from polymer to fullerene is the same for APFO3/[70]PCBM and APFO3/[60]PCBM but somewhat higher for APFO3/[70]BTPF. This qualitatively agrees with the results of fitting of early time TA kinetics (see Table 2), showing that the charge generation times for APFO3/[70]PCBM and APFO3/[60]PCBM blends are very similar (∼200 fs) and that charge generation in the APFO3/[70]BTPF blend is somewhat faster (∼100 fs). Thus, there is a qualitative agreement between the charge generation rates in the present polymer/fullerene systems and the free energy differences (the driving force, ΔG^0) of electron transfer of the reaction. The high rate of charge generation would require low activation energy for a nonadiabatic reaction, and therefore, the reorganization energy should be of the order of ∼0.6 eV for both blends with the PCBM-type of acceptors and ∼0.8 eV for [70]BTPF. This estimated range of the reorganization energy is higher than the value of ∼0.3 eV reported for conjugated polymers and for complexes of organic dyes and fullerenes.[50−52] A reorganization energy of ∼0.3 eV would result in a substantial activation barrier of ∼3*kT* for [70]PCBM /[60]PCBM acceptors and up to ∼8*kT* for the [70]BTPF. Also, because of the presence of different fullerene derivatives in the blends studied, variation in the coupling elements cannot be ruled out. The different anchoring group in APFO3/[70]BTPF than in APFO3/[70]PCBM or in APFO3/[60]PCBM may perhaps cause stronger coupling for APFO3/[70]BTPF than for the other two blends and hence lead to faster electron transfer, although the obtained rates are rather close for all blends. Furthermore, the rates of charge generation in all studied blends are quite high, suggesting that a possibility of adiabatic electron passage from the excited APFO3 to a fullerene cannot be excluded.

Charge Recombination. The modeling results (Table 2) show that the first order recombination rate for the 1:1 blend of APFO3/[70]PCBM is very low $(\sim 330\ ns)^{-1}$ compared to the rates for the 1:1 blend of APFO3/[60]PCBM $(\sim 30\ ns)^{-1}$ and the 1:1 blend of APFO3/[70]BTPF $(\sim 7\ ns)^{-1}$. The very broad distribution ($\sigma_3 \approx 43$) of the Gaussian distribution of the first order recombination rate for APFO3/[70]BTPF indicates that the recombination process starts very early for this material compared to the other two blends (Figure 8ii). It is clear that in terms of both mean recombination rate and width of distribution, the geminate recombination depends strongly on the type of fullerene derivative in the studied polymer/fullerene blends and is slowing down in going from APFO3/[70]BTPF to APFO3/[60]PCBM to APFO3/[70]PCBM. If the relatively slow recombination occurs in a single reaction step, a nonadiabatic Marcus approach to analyze this charge transfer reaction should be applicable. Assuming that the fast charge generation is a barrierless nonadiabatic reaction whereas recombination is retarded by an activation barrier of the reaction, the reorganization energy of the recombination can be estimated as $\lambda = 0.69$ eV for APFO3/[70]PCBM, $\lambda = 0.7$ eV for APFO3/[60]PCBM, and $\lambda = 0.59$ eV for APFO3/[70]BTPF blends, respectively. All recombination reactions appear to have high activation barriers; therefore, only small variations of λ are needed to account for the observed differences in the recombination rates. These reorganization energies are close to but not equal to the values required for a barrierless charge generation reactions. Also, the reorganization energy for the APFO3/[70]BTPF blend appears somewhat smaller than that for the other blends, opposite the requirements for assumingly barrierless charge generation. Yet another inconsistency of this analysis is that, contrary to the estimates, one would expect the two C_{70} acceptors to have more similar reorganization energies than different fullerenes acceptors (i.e., [60]PCBM vs [70]PCBM), although variation of reorganization energies for all blends is not great. It is also worth mentioning that electronic coupling solely should not be responsible for the difference in rates, since large rate variation is observed for the two PCBM-type acceptors with the same anchoring group. Thus, a Marcus description of the charge recombination process in the studied polymer/fullerene blends does not seem completely straightforward, but it should at the same time be realized that only small variations in reorganization energy and free energy changes will generate large differences in rates. The problem with using the Marcus picture for a single-step electron transfer to describe charge recombination in a BHJ blend is, as we will discuss below, of more fundamental nature.

The Marcus picture used above describes a single-step electron transfer process with a well-defined donor−acceptor distance. However, in a solid BHJ film charges do not necessarily reside at the positions they were formed after forward ET but rather migrate through the polymer and fullerene networks to new sites away from where they were formed. This separation process definitely has to occur in a functioning solar cell. Does it also occur in a BHJ film without an internal electric field? If first order geminate recombination occurs from a charge separated state, it probably involves a multiple step process and the Marcus equation in eq 1 cannot be directly applied. In that

(48) Marcus, R. A. *J. Chem. Phys.* **1956**, *24*, 966–978.
(49) Marcus, R. A.; Sutin, N. *Biochim. Biophys. Acta* **1985**, *811*, 265–322.
(50) Imahori, H.; Yamada, H.; Guldi, D. M.; Endo, Y.; Shimomura, A.; Kundu, S.; Yamada, K.; Okada, T.; Sakata, Y.; Fukuzumi, S. *Angew. Chem., Int. Ed.* **2002**, *41*, 2344–2347.
(51) Mi, S. Z.; Lu, N. *J. Mol. Struct.: THEOCHEM* **2010**, *940*, 1–5.
(52) Ran, X. Q.; Feng, J. K.; Ren, A. M.; Li, W. C.; Zou, L. Y.; Sun, C. C. *J. Phys. Chem. A* **2009**, *113*, 7933–7939.

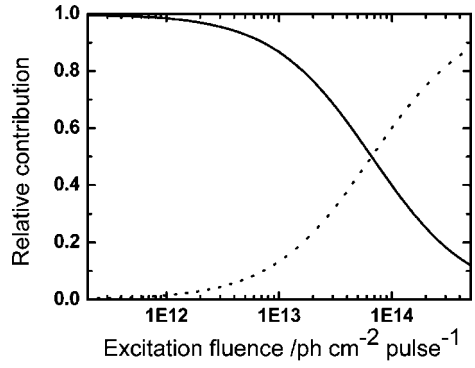

Figure 9. Relative contribution of first order (solid line) and second order (dotted line) recombination processes at various excitation fluence for APFO3/[70]PCBM 1:1 blend. The excitation fluence axis (abscissa) is logarithmic.

event, electron−hole geminate recombination would be preceded by multiple electron or hole transfers within the fullerene or polymer networks.

In order to judge whether charge mobility and varying electron transfer distance in different polymer/fullerene blends are an integral part of the measured rates of the first order recombination, the electron−hole distance at the time of recombination in a charge pair is needed. We can obtain this from a comparison of the relative contributions of first order (geminate) and second order (nongeminate) recombination. For that, we integrate over the whole time scale the parts of the recombination kinetics that come from first and from second order processes separately and then compare the results for various excitation fluences. This can be easily performed, since we know, from the kinetic fitting at all intensities, the time dependence of geminate and nongeminate recombination individually. The two curves in Figure 9 show how the contributions of the two modes of recombination vary with excitation intensity for APFO3/[70]PCBM (the corresponding data for the other two blends are shown in Supporting Information Figures SI4 and SI5). We also assume that in the inhomogeneous sample there is a characteristic distance between the charges after their separation that determines the first order process. The second order recombination has to be dependent on the average distance between charges or, under the assumption of 100% charge generation yield, between excitations, which can be determined from the number of photons absorbed by the sample. We can therefore estimate the characteristic electron−hole distance of the first order process as the average distance between excitations at the fluence when both recombination channels contribute equally (crossing point between the two curves in Figure 9). Figure 9 shows that for APFO3/[70]PCBM the two different modes of recombination contribute equally to the overall recombination at an excitation density of $\sim 7 \times 10^{13}$ (photons/cm^2)/pulse. For uniform illumination of the sample this corresponds to an average distance between excitations (and thus charges of different sign in nongeminate recombination) of 4.6 nm. Since first order and nongeminate recombination have the same relative contributions to recombination at this charge density, we know that on average first order recombination occurs at an electron−hole distance of 4.6 nm with a rate of $(330\ \text{ns})^{-1}$ for APFO3/[70]PCBM. The corresponding distances for the other two blends are 3.4 nm for APFO3/[60]PCBM and 1.2 nm for APFO3/[70]BTPF (as obtained from the data in Figures SI4 and SI5). Thus, first order recombination occurs over considerably shorter distance for these two blends, corresponding to faster recombination.

In the context of charge generation we showed above that there is no phase separation in the studied APFO3/fullerene blends; the charge generation time is ultrafast and very similar for all three blends, implying that there is no energy transfer through a neat polymer phase and that charge generation occurs over approximately the same distance for all blends. The consequence of this is that the initial charge separation distance is controlled by size of the fullerene ball ($\sim$0.7 nm) and the polymer unit length ($\sim$1.5 nm). By comparison of these distances with the distances from which charge recombination occurs, it is clear that for AFFO3/[70]PCBM the charges migrate substantially from the moment of photogeneration to recombination. For the APFO3/[60]PCBM the migration distance is smaller and for APFO3/[70]BTPF the charges have hardly moved.

The results discussed above highlight an intriguing aspect of the charge separation and recombination dynamics in a conjugated polymer/fullerene BHJ. On the one hand the photogenerated charges in a charge pair shortly after photogeneration move rapidly apart despite a strong Coulombic attraction, but on the other hand at later times when the electron−hole distance has increased and the Coulomb interaction is weaker, geminate recombination occurs. This suggests that in films in the absence of an internal electric field there is a "force" separating the charges against the Coulomb attraction at early times. However, in films the charges never fully escape the Coulombic interaction but eventually recombine. In an operating solar cell with high IQE the conditions obviously are such that recombination is largely eliminated. An important question to answer is the following: What are these conditions that drive the charges apart against the Coulomb attraction? The present results do not allow us to provide a definite answer, but we note that excess energy deposited to the charges through the absorbed light causes very high initial charge mobility, as has been revealed by ultrafast THz measurements on BHJ blends[53] and electric field induced second harmonic generation in neat polymers.[21] This early time high mobility could facilitate the initial charge separation. This picture of charge separation appears to agree with that suggested by Pensack and Ashbury[54] on the basis of time-resolved infrared measurements on a CN-MEH-PPV/PCBM blend. They conclude that charge separation occurs on a picosecond time scale in a barrierless process assisted by excess vibrational energy supplied by the optical excitation. Matrix elements for electron and hole transfer in combination with charge screening and polarization effects[27] are probably properties that make charge separation and thus recombination material dependent. It appears as a challenge to theory to disentangle how these (and other) effects contribute to yield the observed separation of charges. In the absence of an internal electric field the Coulomb attraction pulls the charges back together to undergo first order recombination on the nanosecond to hundreds of nanoseconds time scale. This recombination is strongly dependent on the material and the rate determined by how far the charges have separated.

The discussion above of charge generation, separation, and recombination in polymer/fullerene bulk heterojunctions leads to the following picture: Photoexcitation of the polymer results in generation of a bound polaron pair with a characteristic

(53) Nemec, H.; Nienhuys, H. K.; Perzon, E.; Zhang, F. L.; Inganas, O.; Kuzel, P.; Sundstrom, V. *Phys. Rev. B* **2009**, *79*, 245326.
(54) Pensack, R. D.; Asbury, J. B. *J. Am. Chem. Soc.* **2009**, *131*, 15986–15987.

formation time of 100−200 fs, somewhat dependent on the driving force for charge transfer. Driven by excess vibrational energy and energetic disorder[24,55] and controlled by electron transfer coupling, polarization, and screening effects,[27] the charges are moving apart under the influence of the mutual Coulomb attraction. In the absence of an internal electric field the Coulomb attraction pulls the charges back together to undergo first order recombination on the nanosecond to hundreds of nanoseconds time scale. This recombination is strongly dependent on the material and the rate determined by how far the charges have separated.

Geminate Charge Recombination in BHJ Films vs Solar Cells. The complete nanosecond time scale geminate electron−hole recombination in BHJ film shows that charges never become completely free but eventually all recombine under the influence of their mutual electrostatic attraction. In order to be extracted from the active material in a solar cell, electron−hole separation has to proceed further beyond that observed here for BHJ films. This separation will necessarily increase the electron−hole distance and therefore make geminate charge recombination slower. In a functional solar cell, this separation process must therefore be a key process and the one competing with geminate recombination. Below we will propose a scenario that may explain how this happens.

At this point it is useful to compare the picture given so far of charge carrier dynamics in a BHJ blend with that proposed for organic solar cells by Bredas et al.[27] in a recent review. According to ref 27, light absorption by the polymer leads to intermolecular charge transfer to a manifold of charge transfer states (CT), followed by charge separation and formation of free charges via a sequence of still interacting charge separated states (CS) (Figure 1 in ref 27). In this scheme the CT states would correspond to what we have termed bound charge pairs (polaron pair),[12] and transfer from hot charge transfer states (CT*) (or high-lying states in an inhomogeneous distribution of CT states) to hot charge separated states (CS*) would correspond to the picoseconds time scale charge separation process discussed above and in ref 12. If internal conversion among the distribution of CT states effectively competes with charge separation, low lying CT states may be populated (or low-lying CT states may be directly populated by charge transfer from the polymer excited state). If these CT states are lower in energy than the CS states, charge separation is an activated process. These CT states are therefore expected to be long-lived and could be the origin of reported red-shifted and long-lived very weak CT emissions.[30,37] Such weak red-shifted emission was also detected for the present blends (Figure 3). Figure 10 shows the results of a time correlated single photon counting experiment detecting the emission from an APFO3/[60]PCBM blend at 826 nm. For comparison, the fluorescence decay at the same wavelength of a neat APFO3 film is shown. The neat APFO3 fluorescence decay is characterized by a nonexponential decay with a dominating short lifetime of 0.94 ns and a weak longer lifetime of 2.3 ns. The emission of the APFO3/[60]PCBM blend has an approximately 5.8 ns very weak decay, assigned to CT emission, in addition to faster components. The very weak CT emission, suggesting a very low population of the low-lying CT states, may explain why these CT states and the corresponding kinetic components have not been resolved in TA measurements (this work and ref 12). TA measurements probe

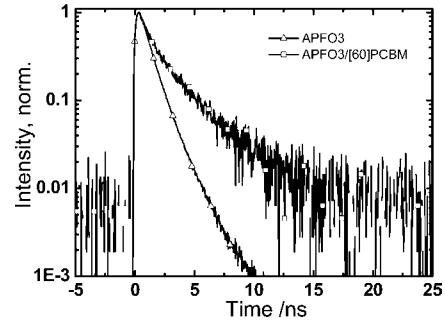

Figure 10. Time correlated single photon counting measurements of fluorescence from a 1:1 APFO3/[60]PCBM blend and neat APFO3 measured at 826 nm.

the majority of CT states (bound electron−hole pairs) that dissociate on the picosecond time scale. The nonexponential nature of the early part of the APFO3/[60]PCBM emission decay in Figure 10, covering the time scale <100 ps to ∼1 ns, may very well be the signature of a distribution of CT states decaying with widely differing rates to separated charges. This is a matter of current investigation.

The charge separated states observed in the BHJ films of our present work corresponds to electron and holes that have moved away from each other to a distance of 1.2−4.6 nm, depending on material, and under the influence of their mutual Coulomb attraction they are recombining on the observed ∼1−100 ns time scale. As already mentioned, in an efficient functional solar cell, recombination obviously cannot occur like in the film. The question to answer is, how does charge recombination change and which are the key factors controlling it? Obtaining these answers may help to achieve more efficient solar cell materials.

Conversion of bound photogenerated charge pairs into free mobile charge carriers is not a very straightforward process considering the strength of Coulomb attraction of a bound pair.[24,55,56] Right after exciton conversion into charges one can estimate the strength of the electric field as $\sim 4 \times 10^8$ V/m for 1 nm distance between charges of different sign when a relative dielectric constant of 3.5 [24] is used. Considering that the internal electric field in a cell under short circuit conditions is of the order of 10^7 V/m, the charges have to be separated by ∼10 nm for the internal field to overcome the Coulomb attraction. The modeling in the current study suggests that the dominant part of the charges remains within this distance even for [70]PCBM with the largest separation. An alternative view on the same problem would be to represent the Coulomb attraction of charges in the form of their binding energy. For the recombination distances determined above, the Coulomb interaction varies between 330 (at 1.2 nm) and 85 meV (at 4.6 nm),[57−59] in close correlation to the values given in ref 24. Thus, the attraction between charges is well above the thermal fluctuation energy, *kT*, explaining that in the absence of an internal electric field eventually all charges recombine. Apparently, such a binding energy would dominate over thermal fluctuations (∼25 meV at

(55) Morteani, A. C.; Sreearunothai, P.; Herz, L. M.; Friend, R. H.; Silva, C. *Phys. Rev. Lett.* **2004**, *92*, 247402.
(56) Arkhipov, V. I.; Heremans, P.; Bassler, H. *Appl. Phys. Lett.* **2003**, *82*, 4605–4607.
(57) Persson, N. K.; Arwin, H.; Inganas, O. *J. Appl. Phys.* **2005**, *97*, 034503.
(58) de Haas, M. P.; Warman, J. M.; Anthopoulos, T. D.; de Leeuw, D. M. *Adv. Funct. Mater.* **2006**, *16*, 2274–2280.
(59) The Coulombic attraction among separated charges was estimated using a relative dielectric constant of 3.7 (an average value of dielectric constants for APFO3, 3.4 (derived from $n = 1.85$ for APFO3 (ref 57)), and PCBM, 4.1 (ref 58)) for all three blends.

room temperature), and as a result, the charges will be pulled together rather than diffuse away in the blend.

Charges embedded in a medium are known to interact with the environment, polarizing the nearest surroundings, in the formation of a polaron. We believe that polaron formation is a process with potential to resolve the problem of Coulomb attraction in BHJ charge recombination. Polaron formation leads to partial screening of charges by deformation of the surrounding or by a superposition of phonons. Thus, Coulomb attraction, and consequently electric field strength and binding energy of photogenerated charges, would decrease in such a process. A polaron size of ~1 nm was estimated for blends[21] and values from 2 to 11 nm have been reported for neat highly conjugated polymers.[60] Thus, formation of polarons with a size of a few nanometers could decrease the Coulomb attraction of separated charges from the high values given above (~85−330 meV) to a *kT* level. However, if formed, polarons are present in both the thin film materials and solar cells, and the static picture of a polaron implicit from the description above does not help us to resolve the conjecture of efficient charge separation and extraction in the presence of electron−hole Coulomb attraction. In other words, the recombination times we observe on the nanosecond to hundreds of nanosecond time scale are the recombination times of polaron pairs. This situation may be resolved by realizing that a polaron is a dynamic feature and that the polarons are mobile within the Coulomb attraction potential. Vibrations of the polymer and fullerene units on which the charges reside as well as vibrations in the environment will result in a fluctuating electric field around the polarons (or alternatively, fluctuating screening). This, in combination with the mobility of the polarons, will give rise to a time dependent attraction between the two constituents of a polaron pair. In the absence of an internal electric field all the fluctuations will be averaged out, and the result is recombination as we observe it in the experiments. It is important to realize that both charges have to be unscreened simultaneously for the Coulomb attraction to result in recombination. In the solar cell on the other hand, the internal electric field acts on each charge separately and imposes directionality. Therefore, the internal electric field is the force that makes it possible for the charges to escape the Coulomb attraction at the moments in time when the fluctuating screening cancels the attraction forces. Also, the internal electric field in the solar cell generated by the charge distribution and the difference in electrode work functions will be diminished because of screening, but the consequence of the fluctuating screening (assumed to be uncorrelated for electron and hole) is that the probability of only one charge being unscreened is (much) higher than both charges being simultaneously unscreened. Apparently, both charges have to be unscreened for Coulomb attraction to pull them toward each other, whereas each unscreened charge is moved to the electrodes by the internal electric field. Also, when only one charge is unscreened, there is no strong interaction to break, and even a very weak internal field can cause significant charge transport. Alternatively expressed, the time averaged polaron screening reduces the Coulomb attraction between electron and hole and positions the system close to the dissociation limit. The field fluctuations present in a real material and the internal electric field present in a solar cell make it possible for the charges to escape from the Coulomb attraction at moments when screening of one of them cancels the attraction. The picture given above is expected to be strongly dependent on properties of the BHJ material; i.e., different polymers have different charge mobility and polarizability, giving rise to various degrees of polaron screening. Widely differing recombination times reported for different BHJ[61−64] may be the signature of the suggested scenario. The importance of understanding on the molecular level polarization and screening effects on the charge separation process is pointed out by Bredas et al.[27] in their review. The picture we have proposed of the charge separation/recombination event implies that in a functional solar cell it is the charge separation that outcompetes geminate recombination and rapidly brings the charge pair to a separation distance where recombination becomes so slow that it no longer competes with the microsecond time scale charge extraction.

Table 3. Summary of the Performance of Solar Cells Made from 1:1 Blends of APFO3/[70]PCBM, APFO3/[60]PCBM,[65] and APFO3/[70]BTPF

	APFO3/[70]PCBM	APFO3/[60]PCBM	APFO3/[70]BTPF
J_{sc} (mA cm^{-2})	5.9	3.7	1.4
V_{oc} (V)	1.04	1.09	0.50
FF	0.43	0.35	0.25
η (%)	2.6	1.4	0.2

The picture painted above of the charge carrier dynamics controlling the function of a solar cell suggests that charge mobility translated into efficient charge separation and reflected as slow geminate charge recombination in the BHJ film is a key property for good solar cell performance. The performances of APFO3/[70]PCBM, APFO3/[60]PCBM, and APFO3/[70]BTPF 1:1 blend solar cells are summarized in Table 3. Short circuit current (J_{SC}) and fill factor (FF) are both increasing with a change of the acceptor type of the polymer/fullerene blend solar cell from [70]BTPF to [60]PCBM to [70]PCBM. The open circuit voltage (V_{OC}) for APFO3/[60]PCBM and APFO3/[70]PCBM is almost the same and approximately a factor of 2 higher than for APFO3/[70]BTPF. The power conversion efficiency (η) of the APFO3/[70]PCBM solar cell is 2 times greater than for APFO3/[60]PCBM and 13 times greater than for APFO3/BTPF70. As expected, we see that solar cell efficiency is *increasing* in the order APFO3/[70]BTPF < APFO3/[60]PCBM < APFO3/[70]PCBM, the same order as the *decrease* in first order recombination rate.

Conclusions

We investigated the influence of three different fullerene derivatives on the charge generation and recombination dynamics of polymer/fullerene solar cell blends. Photoexcitation of the polymer results in formation of a bound electron−hole pair, which in APFO3/[70]PCBM and APFO3/[60]PCBM occurs with very similar rates (~200 fs)$^{-1}$ and is somewhat slower than in APFO3/[70]BTPF (~100 fs)$^{-1}$. This difference agrees qualitatively with the trend in driving force estimated from the LUMO energies of the polymer and fullerene derivatives. However, the high rates of charge generation, in combination

(60) Meisel, K. D.; Vocks, H.; Bobbert, P. A. *Phys. Rev. B* **2005**, *71*, 205206.
(61) Nogueira, A. F.; Montanari, I.; Nelson, J.; Durrant, J. R.; Winder, C.; Sariciftci, N. S. *J. Phys. Chem. B* **2003**, *107*, 1567–1573.
(62) Nelson, J.; Choulis, S. A.; Durrant, J. R. *Thin Solid Films* **2004**, *451*, 508–514.
(63) Offermans, T.; Meskers, S. C. J.; Janssen, R. A. J. *J. Chem. Phys.* **2003**, *119*, 10924–10929.
(64) Savenije, T. J.; Kroeze, J. E.; Wienk, M. M.; Kroon, J. M.; Warman, J. M. *Phys. Rev. B* **2004**, *69*, 155205.
(65) Andersson, L. M.; Zhang, F. L.; Inganas, O. *Appl. Phys. Lett.* **2007**, *91*, 071108.

with previously estimated values of the reorganization energy, may indicate that adiabatic electron passage from the excited APFO3 to a fullerene has to be considered for this reaction step. On the basis of a comparison of the relative contributions of geminate and nongeminate charge recombination as a function of excitation density, we can obtain the electron−hole distance from which geminate recombination occurs. This shows that charges separate up to several nanometers, with how much depending on material, from the moment they are formed to the onset of charge recombination. We suggest that the charge separation process is facilitated by high charge mobility at early times after the photoexcitation and that it is driven by excess vibrational energy and energetic disorder and controlled by electron transfer coupling under the influence of the attractive Coulomb interaction between electron and hole. In the absence of an internal electric field the Coulomb attraction eventually pulls the charges back together to undergo first order geminate recombination on the time scale of nanoseconds to hundreds of nanoseconds. The observed variation of charge recombination rate for the different blends matches measured power conversion efficiencies of solar cells based on the same materials. Charge separation rather than their extraction is suggested as a process to outcompete geminate recombination in a functional solar cell. Decrease of Coulomb attraction as a result of medium polarization,[27] polaron formation and its dynamic nature resulting in time fluctuating screening, is considered as a mechanism that may allow conversion of bound photogenerated charges into separated mobile charge carriers in a solar cell.

Acknowledgment. This work was performed with the help of funding from the Swedish Research Council (VR), the Swedish Energy Agency (STEM), the Swedish Foundation for Strategic Research (SSF) through the Center of Organic Electronics, the Crafoord Foundation, and the Knut and Alice Wallenberg Foundation. F.L. acknowledges the support from Ministerio de Ciencia e Innovación of Spain, FEDER funds (Project CTQ2007-63363/PPQ and Consolider Project HOPE CSD2007-00007). We thank Prof. I. Scheblykin for advice in designing the time-resolved fluorescence setup and M. Bilal Akhtar and M. Bilal Siddique for their help with the time-resolved fluorescence measurements.

Supporting Information Available: TA kinetics for APFO3/[70]PCBM 1:1 blend at various excitation wavelengths, TA kinetics at various excitation fluences and fitting results of TA kinetics for a 1:1 blend of APFO3/[70]BTPF, relative contribution of first order and second order recombination processes at various excitation fluences for 1:1 blends of APFO3/[70]BTPF and APFO3/[60]PCBM, and turnover rates for all the processes in Scheme 1 for the 1:1 APFO3/[70]PCBM blend. This material is available free of charge via the Internet at http://pubs.acs.org.

JA104786X